Superposed epoch analysis of the dayside ionospheric response to four intense geomagnetic storms

A. J. Mannucci,[1] B. T. Tsurutani,[1] M. A. Abdu,[2] W. D. Gonzalez,[2] A. Komjathy,[1] E. Echer,[2] B. A. Iijima,[1] G. Crowley,[3] and D. Anderson[4]

[1] Prompt daytime ionospheric responses are presented for the following four intense geomagnetic storms: 29 October 2003, 30 October 2003, 20 November 2003, and 7 November 2004. We perform a superposed epoch analysis of the storms by defining the start time of the epoch when the Kan-Lee interplanetary electric field (proportional to the reconnection electric field) first reaches 10 mV/m during a period of continuously southward B_z. Measurements from the GPS receiver onboard the CHAMP satellite at 400 km altitude indicate significant low- to middle-latitude daytime total electron content (TEC) increases above the satellite within $1–2$ h of the defined start time for three of the storms ($\sim$1400 local solar time). The 20 November 2003 data follow a different pattern: the largest TEC increases appear several hours ($\sim$5–7) following the interplanetary magnetic field B_z event onset. TEC data obtained from ground-based GPS receivers for the November 2003 storm tend to confirm a "late" TEC increase for this storm at $\sim$1400 LT. Estimates of vertical plasma uplift near the equator at Jicamarca longitudes ($\sim$281 E) using the dual-magnetometer technique suggest that variability of the timing of the TEC response is associated with variability in the prompt penetration of electric fields to low latitudes. It is also found that for the November 2003 magnetic storm the cross-correlation function between the SYM-H index and the interplanetary electric field reached maximum correlation with a lag time of 4 h. Such a large lag time has never been noted before. The long delays of both the ionosphere and magnetosphere responses need to be better understood.

Citation: Mannucci, A. J., B. T. Tsurutani, M. A. Abdu, W. D. Gonzalez, A. Komjathy, E. Echer, B. A. Iijima, G. Crowley, and D. Anderson (2008), Superposed epoch analysis of the dayside ionospheric response to four intense geomagnetic storms, *J. Geophys. Res.*, *113*, A00A02, doi:10.1029/2007JA012732.

1. Introduction

[2] Recent satellite and ground-based data have elucidated the prompt daytime ionospheric response to intense geomagnetic storms ("superstorms") [*Mannucci et al.*, 2005a; *Tsurutani et al.*, 2004; *Lin et al.*, 2005a]. Total electron content (TEC) data obtained from the ground and from space have shown the hemispheric-scale nature of the response in more detail than has been possible with past data sets that identified fundamental causative mechanisms [*Mendillo*, 2006]. The prompt dayside ionospheric response during the main phase of geomagnetic storms can be understood as a consequence of prompt penetration electric fields (PPEF) that are themselves the consequence of solar wind interaction with the magnetosphere. The resulting vertical and poleward plasma drift in the ionosphere due to east-west directed electric fields leads to large magnitude increases in dayside TEC at low to middle latitudes. The physical mechanisms leading to TEC increases during daytime are at least partially understood [*Huba et al.*, 2005; *Lin et al.*, 2005b; *Verkhoglyadova et al.*, 2007; *Tsurutani et al.*, 2007]. These recent modeling studies suggest that PPEF is an important factor in dayside hemispheric-scale TEC changes that can occur within $2–3$ h after the sudden commencement phase of the geomagnetic storm.
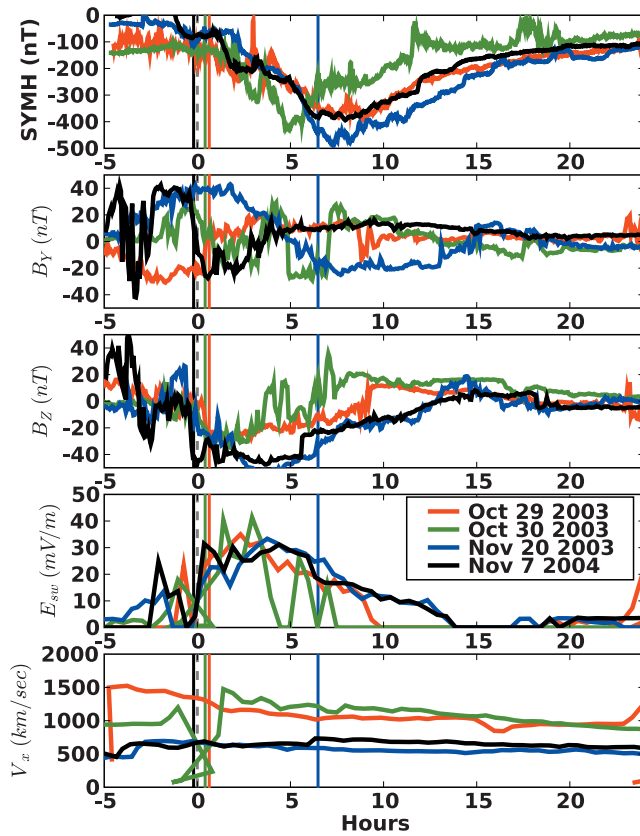
[3] The ionospheric response to prompt penetration electric fields offers the opportunity to study solar wind-ionosphere coupling as it affects the middle- and low-latitude ionosphere. In principle, the dayside ionosphere should begin to respond within minutes after solar wind conditions lead to PPEF at low latitudes. Theory suggests that Region 1 field-aligned currents and their horizontal closure currents [*de la Beaujardiere et al.*, 1993] play an important role in generating global ionospheric electric fields and that these currents respond directly to solar wind conditions such as the orientation and magnitude of the interplanetary magnetic

[1]Jet Propulsion Laboratory, California Institute of Technology, Pasadena, California, USA.
[2]National Institute for Space Research, Sao Jose dos Campos, Sao Paulo, Brazil.
[3]Atmospheric and Space Technology Research Associates, San Antonio, Texas, USA.
[4]Space Environment Center, Cooperative Institute for Research in Environmental Science, University of Colorado, Boulder, Colorado, USA.

Figure 1. Measured solar wind parameters and SYM-H index for the four superstorms in superposed epoch format. The gray vertical line indicates the starting time of the storm epoch, and the colored vertical lines correspond to the time when significant total electron content (TEC) changes are first observed.

field, the ion velocity, and dynamic pressure. The focus of this paper is intense geomagnetic storms associated with long-duration (>1 h) southward oriented interplanetary magnetic fields that cause the largest geoeffective responses [*Gonzalez and Tsurutani*, 1987]. Significant changes in TEC have been reported after ~1–2 h of intense solar wind forcing [*Mannucci et al.*, 2005a, 2005b; *Tsurutani et al.*, 2004; *Mendillo*, 2006; *Abdu*, 1997].

[4] In this paper we use a common-epoch analysis to study large-scale ionospheric response to four of the most intense "superstorms," as measured by *Dst*, of the 2001–2004 period near solar maximum and its declining phase. In section 2, we compare the time histories of the four storms as measured by solar wind parameters and the ring current response (SYM-H index). In section 3, we show evidence for significant variation in ionospheric response. Factors contributing to the variation in ionospheric response are discussed in section 4. Conclusions and suggestions for further study are discussed in section 5.

2. Time Histories of Four Superstorms

[5] The time histories of the solar wind parameters and geomagnetic response for the storms included in this study are shown in Figure 1 in "superposed epoch" format:
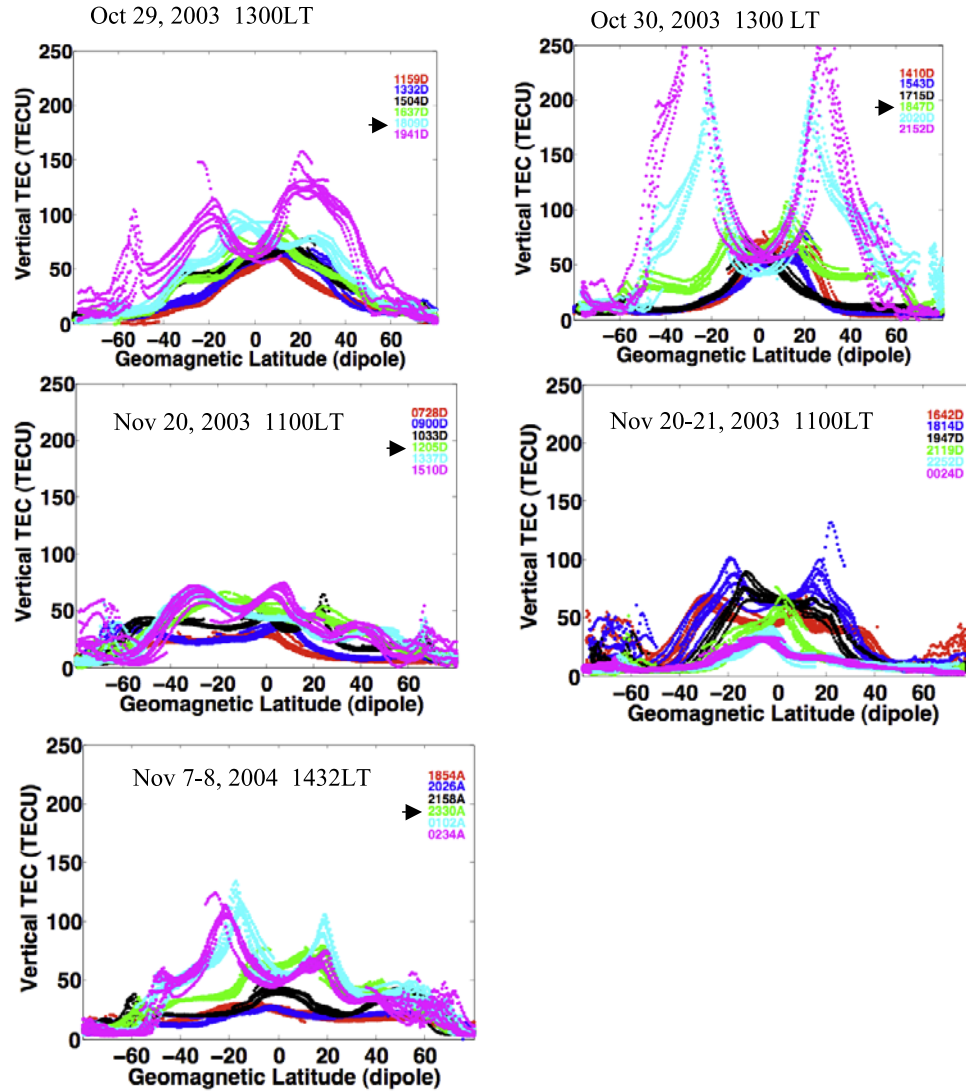
SYM-H index (1-min values) and interplanetary parameters B_y, B_z (GSM coordinates), interplanetary electric field E_{SW}, and solar wind speed toward Earth (Vx, GSM). We define a common starting time for the storm epochs focusing on a parameter related to the reconnection electric field at the magnetopause, computed as $E_{sw} = |V_x| B_T \sin^2 (\psi/2)$ [*Kan and Lee*, 1979]. V_x is the earthward velocity (GSM coordinates), B_T is the component of B perpendicular to the Earth-Sun line ($B_T = \sqrt{B_y^2 + B_z^2}$), and ψ is the "clock angle" of the interplanetary magnetic field (rotation angle in the y-z plane; $90 < \psi < 270$ is assumed). Theoretical considerations and empirical formulations suggest that the cross polar cap potential should be related to the above formulation for E_{sw} [*Rothwell and Jasperse*, 2006; *Sonnerup*, 1974; *Fedder and Lyon*, 1987]. The fourth panel in Figure 1 is E_{sw} with positive sign when E_{sw} is in the "geoeffective" negative y direction (GSM), corresponding to $B_z < 0$. E_{sw} is set to zero when oriented in the positive direction ($B_z > 0$). The close association between PPEF and the cross polar cap potential drop [*Siscoe et al.*, 2002; *Nopper and Carovillano*, 1978] suggests that the common epoch analysis is reasonably based on E_{sw} to determine the epoch start time.

[6] The gray vertical line shown in Figure 1 defines the starting time for each storm epoch as determined by a common criterion applied to all four storms. All of the superstorm events are associated with a long-duration southward interplanetary magnetic field (IMF) B_z of significant magnitude. The starting time of the epoch (vertical line) is set to zero when E_{sw} reaches 10 mV/m before reaching 30 mV/m or more, without changing sign as E_{sw} proceeds from 10 to 30 mV/m. The value of 10 mV/m is generally associated with extreme storms, and it is approximately 1/4–1/3 of the maximum value reached for the storms. A larger value of 30 mV/m is eventually reached which is close to the maximum value for all the storms. The storms all exhibit similar time histories in the progression from 10 mV/m to 30 mV/m, although the fluctuations in interplanetary electric field (IEF) distinguish the different cases in detail. Table 1 lists the universal times when the storm epochs begin. The focus of this study is the delay of the ionospheric response relative to the IEF time series. The similarity of the time series suggests it is reasonable to intercompare the TEC responses in light of the "onset" time as defined here (E_{sw} threshold at 10 mV/m). Choice of other threshold values to define storm onset will change the absolute time elapsed between the epoch start and the ionospheric response. However, it will not significantly change the conclusions regarding how the ionospheric response differs in time between the four storms.

[7] Another timing consideration is the solar wind speed that controls the delay between magnetopause arrival time

Table 1. Storm Onset Times

Date	Interplanetary Electric Field, UT	Total Electron Content, UT
29 Oct 2003	1731	1809
30 Oct 2003	1822	1847
20 Nov 2003	1122	1751
7 Nov 2003	2242	2230

Figure 2. Vertical TEC estimates above the CHAMP satellite for the four superstorms as a function of universal time (UT). UT of the traces is indicated in the upper right corner of each panel ("A" represents passes ascending in latitude; "D" represents descending passes). Each color corresponds to a single satellite pass. Multiple traces per pass are obtained as multiple GPS satellites are tracked simultaneously. The arrowheads indicate the first pass following the epoch start time based on E_{sw}.

and the time when the interplanetary magnetic cloud properties are measured by ACE. We assume a fixed magnitude of 1.4×10^6 km as the distance between ACE and the magnetopause. All geophysical quantities have been shifted in time to reflect this distance divided by the solar wind speed measured at ACE. The distance from ACE to the magnetopause varies for each storm period but the range of variation is small: 1.44×10^6, 1.48×10^6, and 1.50×10^6 km for the October 2003, November 2003, and November 2004 storm periods, respectively. Using a fixed value of 1.4×10^6 km results in an error of at most 4 min for a speed of 500 km/s, which is not significant for our study.

[8] The velocities used in Figure 1 and subsequent analysis for the 29 and 30 October 2003 storms required special processing due to their extremely large magnitudes [*Skoug et al.*, 2004]. For those 2 days these data are only available at a low cadence of 30 min versus 1 min for the 2

other days in this study. The sudden increase in speed near hour zero in Figure 1 creates a temporary "reverse time" artifact for 30 October as the time shift from ACE is applied to the data with this low cadence.

3. Ionospheric Response

[9] In Figure 2 we present a time history of ionospheric responses to the four geomagnetic storms considered in this study. We use observations from the CHAMP satellite that carries a zenith-viewing Global Positioning System (GPS) antenna [*Mannucci et al.*, 2005a; *Tsurutani et al.*, 2004]. GPS signals received from this antenna measure the total electron content between the CHAMP satellite GPS receiver at 400 km altitude and the GPS satellites in view. The GPS satellites orbit at 20,200 km altitude, far above the ionosphere and often outside the plasmasphere. Several satellites

are tracked by CHAMP simultaneously (typically 6–10 satellites) with a TEC data cadence of 10 s. The satellite speed is approximately 7 km/s relative to the ground.

[10] This study is focused on daytime. The dayside local times for the satellite equatorial crossings are indicated in Figure 2. A useful property of the satellite data is that the multiple passes for each storm all acquire data at the same local time at each latitude point. The latitudinal profile of the TEC response can be studied for a single local time at the cadence of the orbit (∼100 min).

[11] The multiple time series plotted in each panel of Figure 2 represent measurements obtained from the CHAMP GPS receiver for consecutive daytime passes of the satellite. Each color corresponds to a satellite pass traversing varying longitudes but fixed local time. We plot the electron content measured by the satellite during a single ascending or descending pass across the latitude range shown. The universal time of the pass shown in the legend corresponds to the time the satellite traverses within ±1° of the geographic equator. The multiple traces of a single color correspond to TEC measured along the lines of sight to multiple GPS satellites being tracked during the pass. Slant measurements obtained above 10 degrees elevation are scaled to estimate vertical TEC above the satellite altitude, using a geometric factor derived by assuming the plasma occupies a spherical shell ionosphere of uniform density and 700 km thickness above the CHAMP altitude. Errors in this scaling due to the actual electron density profile and due to horizontal electron density gradients cause the multiple traces of a single color to deviate from each other.

[12] Increases in TEC during daytime are expected in the early phases of superstorms [*Mannucci et al.*, 2005a; *Fuller-Rowell et al.*, 1997; *Prölss*, 1997; *Fejer*, 2002; *Mendillo*, 2006; *Tanaka and Hirao*, 1973; *Abdu*, 1997]. Increased TEC after the event time is evident for all four storms shown in Figure 2, although the magnitudes of the increases vary significantly. For the two Halloween storms (2003) and the 2004 storm shown, a detectable TEC increase is observed starting within one or two orbits of the "event times" defined in Table 1. The 20 November 2003 storm follows a different pattern. Several hours and orbital periods elapse before a clearly distinguished TEC increase is observed similar to that observed for the other three storms. The time history of E_{sw} for all four storms is similar, as is the characteristic of strongly southward IMF following the defined "event time." The apparent delay in the 20 November 2003 TEC response is the subject of discussion in section 4.

4. Discussion

[13] The CHAMP data of 20 November 2003 suggests a different ionospheric response following the southward B_z IMF conditions compared with the three other superstorms studied here. The peak amplitude of the TEC above CHAMP altitude does not increase significantly within 100–200 min (1–2 orbital periods) of the time when large-magnitude B_z south conditions impinge on the magnetopause. If the PPEF is closely linked causally and temporally to the IEF and E_{sw} [*Kelley et al.*, 2003; *Huang et al.*, 2005], then the expectation is that ionospheric TEC increase early in the geomagnetic storm can be organized by
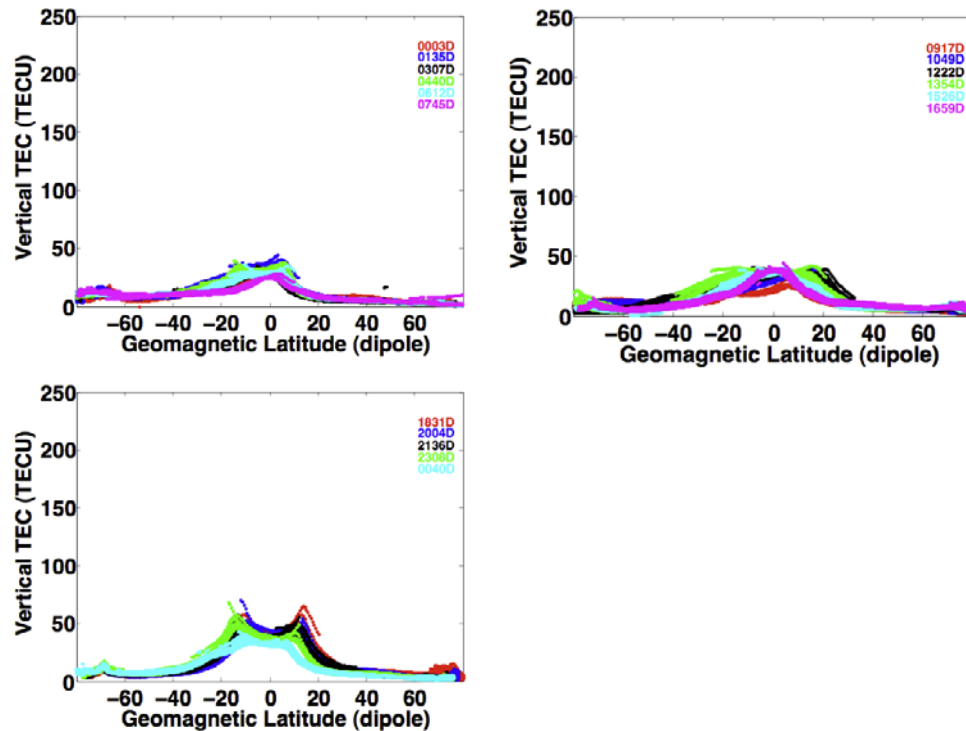
the time history of the IEF. The time histories of IEF for all four superstorms follow a similar pattern of rise and decay (see E_{sw} in Figure 1) and reach similar peak magnitudes.

[14] The TEC variations shown in Figure 2 as a function of UT are probably not predominantly a longitudinal effect occurring as the satellite orbit traverses progressively western longitudes due to Earth rotation. Longitudinal variability can be assessed for quiet conditions using data from 18 November 2003 and shown in Figure 3. Traces at similar UT to the storm day (20 November 2003; Figure 2) traverse similar longitudes to the storm day at the same 1100 solar local time. Although the traces display variability, it is clear that the storm time behavior is qualitatively different than the quiet time behavior. We therefore assume that the large pass-to-pass TEC changes seen in Figure 2 are due to temporal evolution caused by the dynamic changes that occur during a geomagnetic storm.

[15] The CHAMP local time is earlier (1100 LT) for 20 November 2003 than for the other superstorms (1300 LT and 1432 LT). Reduced photoionization occurs during morning local times compared to afternoon local times, reducing the magnitude of the expected TEC increase for a given PPEF applied at morning local times. (The prestorm equatorial anomaly is significantly less developed at 1100 LT than in the afternoon local times). There is also the possibility of local time dependence of the penetration electric fields at low latitudes, as well as storm-to-storm variations of the local time response. Using a coarse global ionospheric conductivity model, *Nopper and Carovillano* [1978] calculated the local time dependence of the PPEF. There is no indication from this calculation that PPEF should differ significantly between 1100 and 1300 LT. The results of a TIEGCM simulation by *Richmond et al.* [2003] also show comparable intensity of the PPEF is expected at these local times.

[16] To investigate the local time behavior of the 20 November 2003 TEC response, we have acquired and processed TEC data available from the global network of ground-based GPS receivers placed world-wide primarily for geodetic purposes [*Komjathy et al.*, 2005]. The ground-based TEC can be used to study the UT history of the TEC at a different local time than available from CHAMP data. The presence of ocean and lack of uniform receiver spacing creates significant latitudinal gaps in the ground-based data compared to the CHAMP zenith TEC data, but the timing of large TEC increases in the low- to middle-latitude regions can be discerned despite these gaps due to the expected broad spatial extent of the response.

[17] Figure 4 shows the TEC from a subset of the ground-based GPS receiver global network after calibration for interfrequency biases and scaling to vertical raypath direction [*Mannucci et al.*, 1998, 1999]. Data from 1200 to 1400 local time are averaged and plotted versus latitude for universal times in the range of interest. Although the coverage has gaps, Figure 4 shows there is sufficient data to reconstruct a partial latitudinal profile of TEC similar to what is available with more completeness above the CHAMP satellite at 400 km altitude. These postnoon data agree with the 1100 LT data from CHAMP in this respect: significant TEC increases are observed more than 6–7 h from the epoch starting time of 1122 UT. The TEC increases are observable for the 1814 UT traces and become
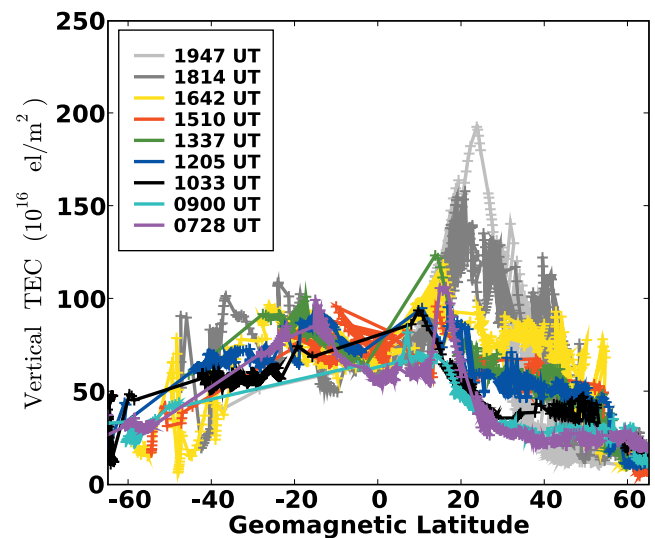
Figure 3. CHAMP vertical TEC for 18 November 2003 corresponding to quiet geomagnetic conditions. Format is similar to Figure 2.
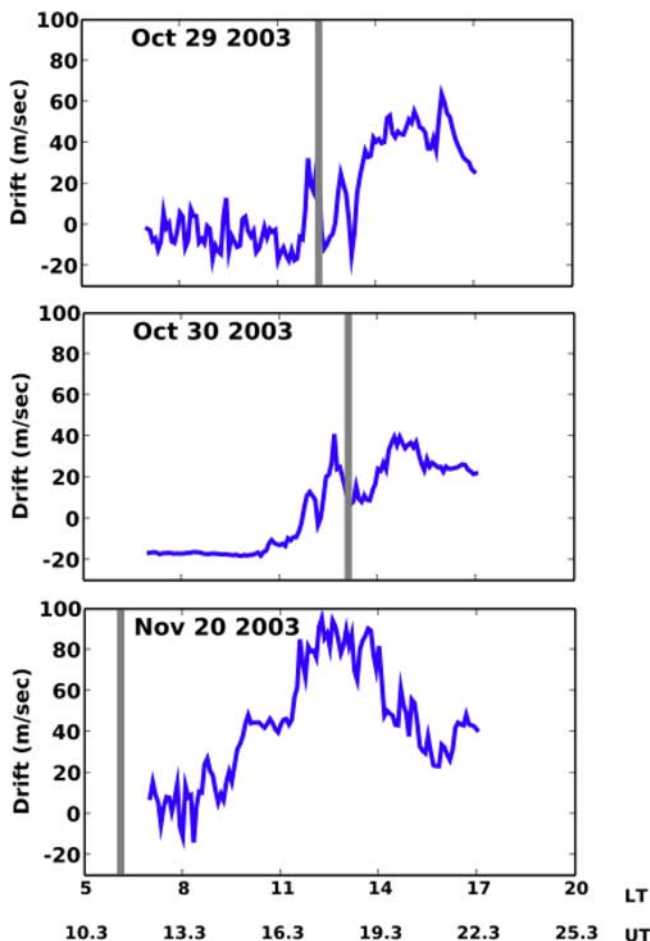
pronounced by 1947 UT. This suggests that the timing of the TEC response for the 20 November 2003 storm is consistent across a broad range of local times (1100 LT to 1300 LT at least).

[18] The preceding discussion is based to some degree on an arbitrary definition of a ''storm epoch'' based on the time that the interplanetary electric field E_{sw} reaches a prescribed value of 10 mV/m. It is reasonable to consider whether another criterion used to define the epoch starting time would result in a more consistent ionospheric behavior across the four superstorms. Insight into this question can be gained by working backward from the time when the significant TEC change is detected. In all four superstorms studied here, a beginning time associated with significant TEC changes can be identified within ±1 h. These times are listed as the third column in Table 1. For the October 2003 and November 2004 storm, the time is based on CHAMP data (Figure 2); for the November 2003 storm it is based on ground TEC data (Figure 4). As expected, the time defined from initial TEC increase is coincident with or later than the time based on E_{sw}. We have indicated the TEC increase time as colored vertical lines in Figure 1. From the perspective of a TEC-based ''epoch start,'' the 20 November 2003 event appears distinguished from the other three superstorms. This suggests that the apparent differences among these superstorms are not due solely to the criterion used to determine the ''storm epoch'' based on IEF. The definition of ''TEC change epoch'' of course depends on a subjectively defined criterion for significant TEC increase. The focus of this paper is the TEC increase that appears to be associated with enhanced Equatorial Ionization Anomaly structure [*Mannucci et al.*, 2005a]. This sort of TEC enhancement

appears promptly for the October 2003 storms and November 2004 storms but later for the 20 November 2003 storm. The ionosphere may be modified promptly for the 20 November 2003 storm also, but the characteristics of this prompt modification appear qualitatively different than for the other three superstorms. A late TEC increase is observed for the 20 November 2003 storm which is absent for the other three storms studied here.

Figure 4. Reconstructed latitudinal profiles of ground-based TEC corresponding to 1200–1400 LT for the 20 November 2003 storm. Apex latitude is used, following *Richmond* [1995].
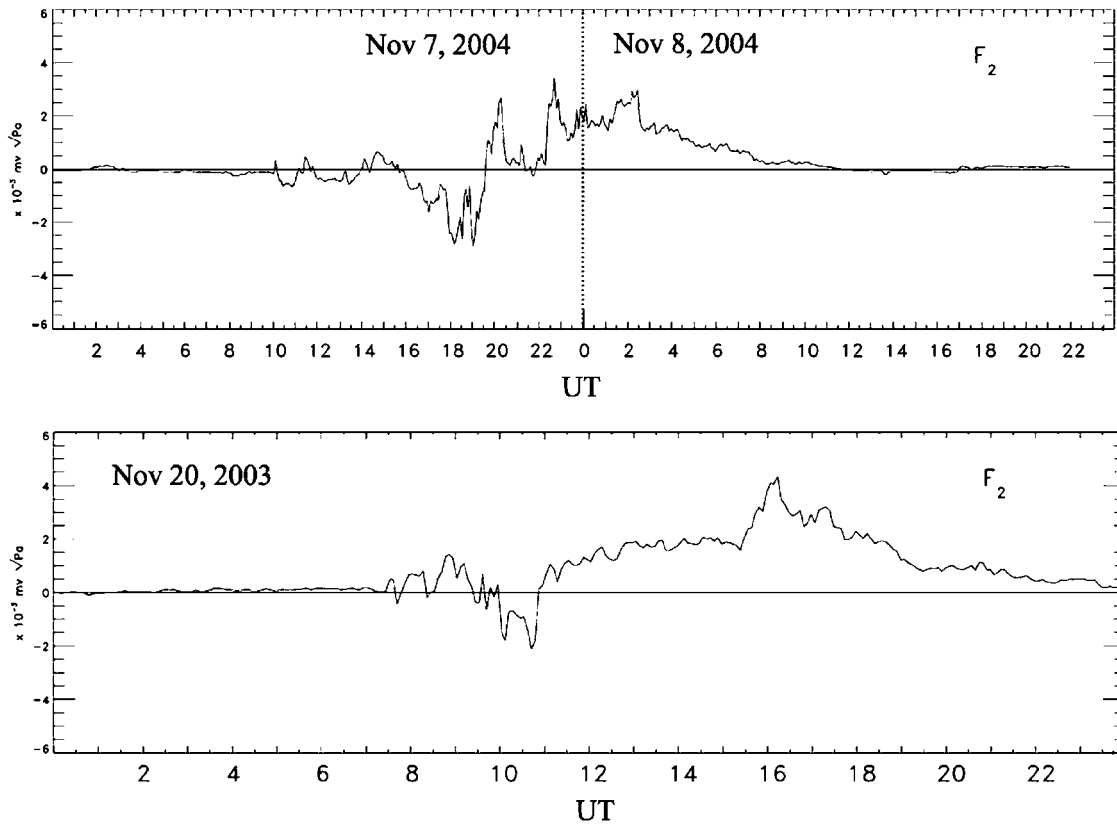
Figure 5. Estimates of vertical $\mathbf{E} \times \mathbf{B}$ drift from the dual-magnetometer technique (positive upward).

[19] To gain insight into the mechanisms responsible for variation of TEC response among the four superstorms, we have examined estimates of equatorial vertical drifts derived from the dual magnetometer technique [*Anderson et al.*, 2002]. Vertical drifts are due to dawn-dusk electric fields penetrating to low latitudes. Data for the superstorms studied here are available from magnetometers near the Jicamarca longitude ($\sim$281 E). This technique is effective during daytime local times (0700–1700 LT). For the 2003 superstorms studied here, the magnetometers were in daytime at universal times relatively near the event epochs. Vertical drift is produced at the equator by zonal electric fields that also modulate the equatorial electrojet. The electrojet current produces a differential magnetic field measured by an on-equator and off-equator magnetometer. *Anderson et al.* [2002] established a quantitative relationship between the magnetometer readings and the vertical drift at Jicamarca longitudes. At this stage in the development of the technique, it is not clear whether the quantitative relationship is the same for all values of the eastward electric field (or vertical drift) and in particular whether the quantitative relationship is the same from quiet conditions through to superstorms. However, we examine the estimated drift velocities here to gain insight into the causes of the TEC variations during the superstorms.

[20] The estimated drift velocities are shown in Figure 5 as a function of local time and UT for the Jicamarca longitude (281E). For the Halloween storms (29 and 30 October 2003) the technique suggests an enhanced electrojet during the storm epochs listed in Table 1. For the November 2003 storm, there does not appear to be an enhancement in the electrojet until much later than the epoch starting time of 1122 UT. Electrojet enhancement appears at $\sim$1500 UT, well past the storm epoch starting time listed in Table 1. Additional enhancement occurs at $\sim$1700 UT, near to the time of the TEC enhancement observed from ground and space data. Nevertheless, for the November 2003 storm the main phase of the geomagnetic storm has started by the epoch time of 1122 UT (see Figure 1). These data suggest that the delayed TEC response for the 20 November 2003 storm is related to the magnitude of the penetration electric field to low latitudes, although definitive conclusions cannot be reached with these drift velocity estimates.

[21] A simple relationship between $\mathbf{E} \times \mathbf{B}$ vertical drift and magnitude of the dayside TEC increase is not established using the estimates from *Anderson et al.*'s [2002] method. *Anderson et al.* [2006] theoretically modeled the low-latitude ionospheric response in the Peruvian longitude sector to the 29 and 30 October and 20 November geomagnetic storms using the daytime $\mathbf{E} \times \mathbf{B}$ drifts pictured in Figure 5 and compared calculated TEC values with observed TEC values in this longitude sector. That study demonstrated the importance of using realistic $\mathbf{E} \times \mathbf{B}$ drift values to model the low-latitude response but also suggested the importance of other physical conditions such as neutral winds, composition, and ion and neutral temperatures to achieve accurate modeling. It is a subject of further study to determine definitely the distinguishing factors that produced the varying TEC response among these three superstorms of 2003.

[22] The largest TEC enhancement is observed for 30 October 2003, which shows the smallest upward drift velocity (peak 40 m/s) of the three storms where the dual-magnetometer technique is applied (Figure 5). The drift velocity for 29 October 2003 reaches higher values ($\sim$60 m/s) although TEC does not reach the large magnitudes of 30 October 2003. We note that independent estimates of the electric field for the 30 October 2003 storm using CHAMP magnetometer data suggest penetration electric fields at the equator of 4 mV/m corresponding to vertical drift velocities of about 120 m/s [*Verkhoglyadova et al.*, 2007; *Tsurutani et al.*, 2007]. These very large electric field values for 30 October 2003 are not reproduced in the dual-magnetometer estimates. For the 20 November 2003 storm, large vertical drift velocities ($\sim$100 m/s) are estimated at $\sim$1700 UT which is several hours following the storm epoch start. Large TEC increases are observed soon after. There is an absence of magnetometer response indicating no equatorial electrojet enhancement for the 20 November 2003 storm until $\sim$1500 UT. This suggests that the late TEC response of the 20 November 2003 is caused by a different relationship between E_{sw} and penetration electric fields for this storm compared to the other two storms shown in Figure 5. The possible delay of a penetration electric field cannot be viewed as a definitive conclusion since unusual conditions in the ionosphere-thermosphere

Figure 6. The F2 index plotted versus universal time (hours) for the storms in 20 November 2003 and 7–8 November 2004. The time axes differ for the two periods.

system [*Yizengaw et al.*, 2006] cannot be ruled out. The TEC response and the vertical drift estimation technique both depend on conditions in the ionosphere-thermosphere system. Prior to the storm epoch starting at ∼1122 UT, other studies of this storm have shown significant storm effects and model studies suggest significant neutral thermosphere composition changes ([O]/[N2] ratio). Thermospheric changes are the result of high-latitude heating and changes in circulation [*Crowley et al.*, 2006; *Meier et al.*, 2005]. A potentially important feature of the 20 November 2003 storm is that relatively mild B_z southward conditions existed prior to the storm onset defined in this paper.
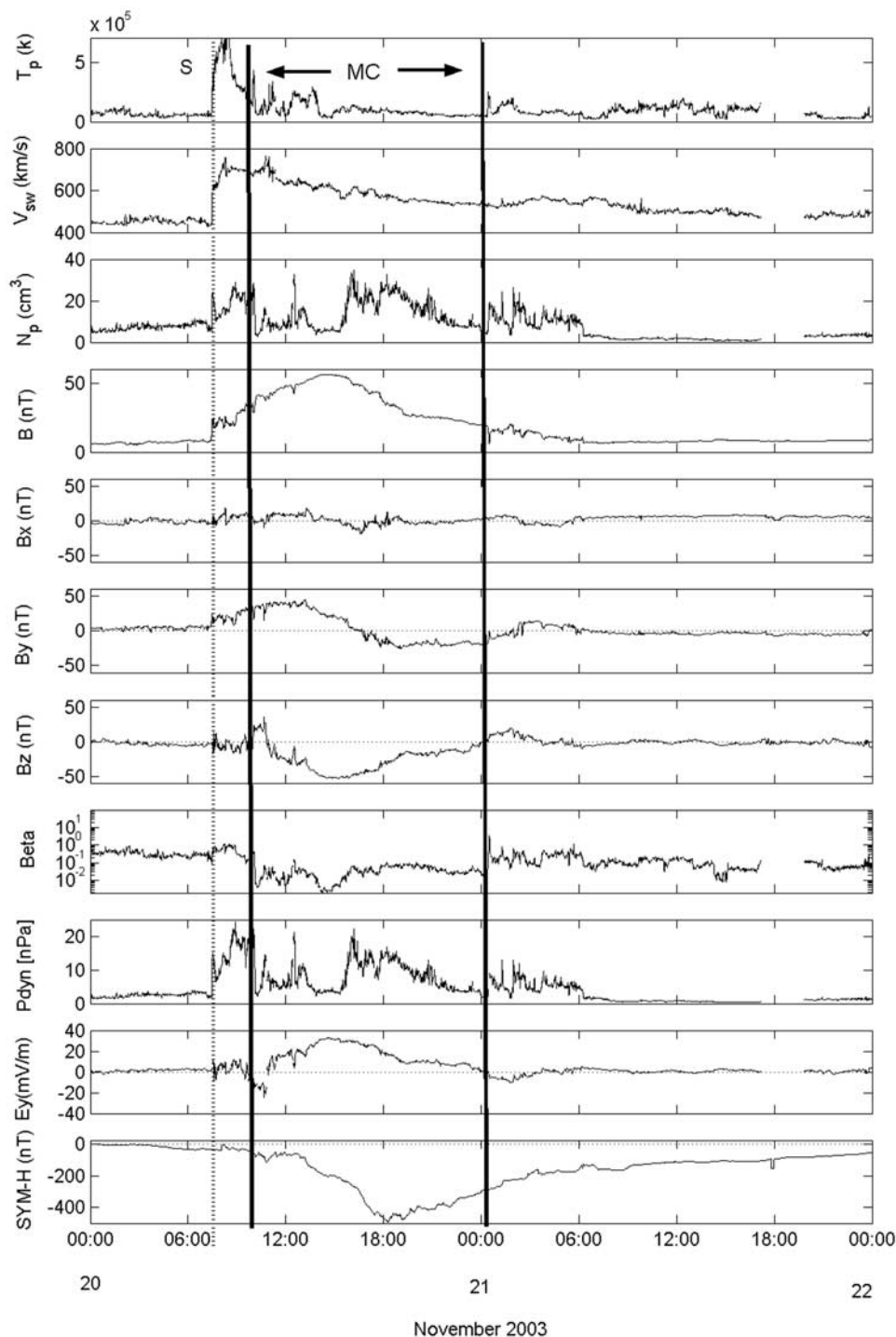
[23] The quantity E_{sw} can be viewed as a special case of the class of coupling functions or scaling relations governing magnetospheric energy transfer [*Gonzalez*, 1990; *Vasyliunas et al.*, 1982]. Solar wind conditions that strongly modulate the energy transfer rate from the solar wind into the magnetosphere are probably contributing factors in the prompt ionospheric response. In particular the solar wind dynamic pressure $\sim \rho V_x^2$ (ρ is the ion density of the solar wind) is expected to modulate the energy transfer and contribute to the magnitude of the polar cap potential drop. We note that for the November 2003 storm the ion density and dynamic pressure increase significantly several hours after B_z southward turning, similarly to the TEC increase. The interplanetary parameters for this storm are shown in Figure 7. Density at the dayside magnetopause increases rapidly from 1600 to 1640 UT (assuming ∼600 km/s solar wind velocity), versus 1751 UT for the first time of TEC increase. The actual TEC increase might have occurred up

to 1 h earlier due uncertainties from the orbital period. The possibility is raised of dynamic pressure playing a role in the TEC increase.

[24] A simplified coupling function that takes dynamic pressure into account is the F2 index [*Gonzalez*, 1990, equation (20)] plotted in Figure 6 for the November storms in 2003 and 2004. The index takes into account the effective increase in magnetopause magnetic field due to the solar wind dynamic pressure and is defined as: F2 = $10^{-3} V_x B_z \sqrt{\rho V_x^2}$. For both of these storms, the timing of the observed TEC increases is soon after the peak F2 value is reached. The peak value is reached for different reasons, however. For the November 2003 storm, the rapid increase in density at ∼1600 UT results in the largest F2 value for the storm. For the November 2004 storm, the peak F2 value is associated with large southward B_z. The solar wind density is actually in decline near to ∼2200 UT when F2 is near its peak. A recent study by *Newell et al.* [2007] concluded that several indices of magnetospheric activity correlate best with a coupling function (designated $d\Phi_{MP}/dt$) that represents the rate at which magnetic flux is opened at the magnetopause, independent of dynamic pressure. An exception is the *Dst* index. The coupling function that correlates best with the *Dst* index is $d\Phi_{MP}/dt$ multiplied by the square root of the solar wind dynamic pressure. Further work is needed to understand the possible dependence of the TEC response to the magnitude and rate of change of solar wind dynamic pressure.

[25] We have found that characteristics of the 20 November 2003 storm are unusual. The relationship of the
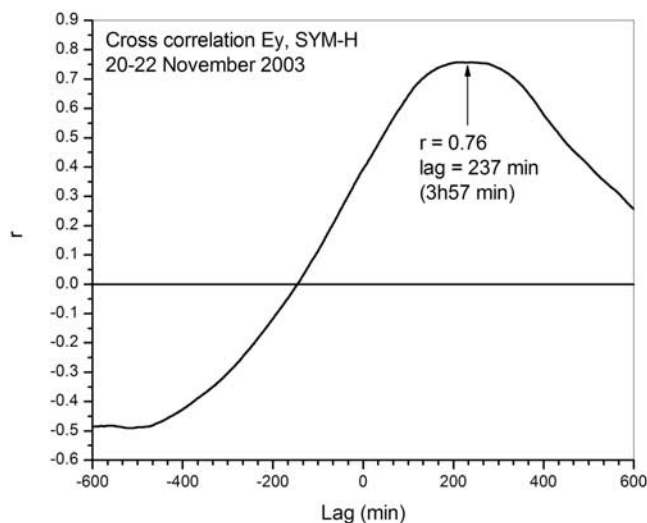
Figure 7. Interplanetary and geomagnetic parameters for the 20 November 2003 storm.

interplanetary parameters and the magnetospheric ring current is given in Figure 7 for the November 2003 storm. The top 10 panels are the solar wind parameters proton temperature, solar wind velocity, density and magnetic field magnitude, the three components of the magnetic field in GSM, the proton beta (proton thermal pressure divided by magnetic pressure), and solar wind ram or dynamic pressure. The bottom panel is the magnetospheric SYM-H parameter (roughly equivalent to *Dst*).

[26] Vertical lines in Figure 7 show three key physical phenomena associated with this solar wind event. The interplanetary shock leading the fast coronal mass ejection (CME) is indicated by an "S." The shock is identified by the large jump in proton temperature, velocity and magnetic field magnitude. The beginning and end of a magnetic cloud (MC) are denoted by solid vertical lines with the designation "MC" given in the proton temperature panel. The MC is identified by the low proton beta. For this event, the interplanetary sheath magnetic field between the shock and

Figure 8. Cross-correlation between interplanetary electric field and *Dst* as a function of lag time.

the start of the MC [*Tsurutani et al.*, 1988] was not southward and therefore did not initiate the main storm phase. The relationship between southward IMFs and magnetic storms has been discussed in detail by *Gonzalez et al.* [1994]. The cause of the magnetic storm is the large southward component of the magnetic cloud. The peak IMF B_z value is -52 nT and the peak SYM-H value is -487 nT.

[27] An unusual aspect of the 20 November 2003 storm relevant to our study is the delay between the magnetic storm and the time history of IMF B_z south. Figure 8 shows a cross-correlation analysis between the interplanetary electric field $E_y = V_x B_z$ and SYM-H, which we use to assess this delay. Before the cross-correlation is computed, the E_y and SYM-H values are each adjusted by a constant to bring their means to zero over the storm period shown. The solar wind speed is greater than 600 km/s, so the delay time between the IMF measurements taken at ACE and arrival at the magnetopause is less than 40 min.

[28] The peak correlation coefficient between E_y and SYM-H is 0.79, a high value as expected. This peak is reached with a lag time of 237 min (3 h, 57 min). The peak values for both the IEF E_y and SYM-H are part of a broad maximum, so the delay between E_y and *Dst* peaks cannot be determined with great precision. This delay is much longer than the mean delay of 78 min found by *Gonzalez et al.* [1989] in a previous study of 10 intense geomagnetic storms (peak *Dst* between -100 and -220 nT) on the rising edge of the 1978–1979 solar cycle maximum. Cross-correlation delays for the storms in that study between *Dst* and interplanetary coupling functions similar to E_y ranged from 0 to 185 min.

[29] The ionospheric response for the 20 November 2003 event is delayed compared to the other three superstorms studied here. The magnetic storm response may also be delayed. Another interpretation for the ionospheric response is that the apparent delay in the response is due to the increased storm time TEC that develops in the "preferred longitude" of the American sector as discussed by *Coster et*

al. [2007] and *Foster and Coster* [2007]. These authors suggest that enhanced TEC during storms may be caused by the unique geomagnetic field structure in the American sector combined with conductivity changes near dusk that create poleward in addition to vertical $\mathbf{E} \times \mathbf{B}$ drift, increasing TEC at low to middle latitudes. However, the data analyzed for this paper (Figure 4) is for 1400 LT where terminator polarization effects are probably not significant, unlike at dusk. If longitude plays a significant role in the TEC response, new explanations are needed for the daytime response of 20 November 2003.

[30] A recent paper by *Basu et al.* [2007] compares ionospheric response at dusk for the 30 October and 20 November 2003 storms. The DMSP satellites record significant ionospheric density depletions at 800 km altitude during these storms. The *Basu et al.* [2007] study reinforces the conclusion that the 20 November 2003 differs from the 30 October 2003 storm with respect to the ionospheric response to solar wind conditions. Basu et al. find that deep electron density depletions at dusk are detected sooner for the 30 October 2003 storm than for the 20 November 2003 storm, when referenced to the time history of B_z (Figures 1 and 6 in that paper). We find in this paper that 30 October 2003 displays similar daytime ionospheric behavior to the 29 October 2003 and 7 November 2004 storms.

5. Conclusions

[31] Studying the ionospheric response of four superstorms to B_z southward turning illustrates that the 20 November 2003 follows a different pattern from the other three. Recent work on PPEF has shown that estimates of electric fields in the low-latitude ionosphere can follow in detail the temporal behavior of the IEF [*Kelley et al.*, 2003; *Huang et al.*, 2005; *Mannucci et al.*, 2005b]. One of the reasons for recent interest in PPEF is that shielding is not always effective in the early phases of intense geomagnetic storms. Understanding and possibly predicting ionospheric behavior during the early phases of geomagnetic storms depends critically on the time history of PPEF. The large ionospheric impact of PPEF values estimated for the 30 October 2003 storm ($\sim$4 mV/m) at low latitudes [*Verkhoglyadova et al.*, 2007; *Tsurutani et al.*, 2007] suggests that it is important to understand the factors that determine penetration electric field magnitudes to low latitudes. Three of the four superstorms in this study follow the qualitative expectation that significant TEC increases follow soon after significant increase of the IEF E_y component (dawn-to-dusk) directed electric field in the interplanetary medium, reinforcing the importance of undershielded penetration electric fields [*Huba et al.*, 2005]. The 20 November 2003 storm appears to follow a qualitatively different pattern. The penetration of the electric field to the ionosphere is delayed an additional $\sim$6 h compared to the other three superstorms. A previous study [*Gonzalez et al.*, 1989] of the relationship between solar wind conditions and geomagnetic response found that the *Dst* peak response is usually delayed from the IEF by about 1 h, as measured by the lag time in the cross-correlation function between *Dst* and IEF. Up to 3 h was observed for one case (10 storms total were included in the study). For the 20 November 2003 storm the corresponding lag time is 4 h. Thus the

relationship between ionospheric response, interplanetary conditions and geomagnetic response appears to be anomalous for 20 November 2003 superstorm. We note that the correspondence between E_{sw} magnitude and TEC increase does not appear to follow a clear quantitative pattern for these four superstorms. Further observations and modeling are required to understand quantitatively the magnitude of the TEC response.

[32] Global ionospheric storms are determined by the time history of solar wind conditions and preexisting and evolving conditions within the ionosphere, thermosphere, and magnetosphere. The plasma structure of the solar wind largely determines the time evolution of the magnetospheric drivers of the ionosphere-thermosphere response. It will be instructive to compare output from models that couple the magnetosphere, thermosphere, and ionosphere in response to solar wind drivers. Such models currently exist at various stages of development. These models may provide clues to the physical mechanisms responsible for the variation of TEC response among these storms or they may clarify where physical understanding is still lacking. Comparisons with coupled models are currently in progress.

References

Abdu, M. A. (1997), Major phenomena of the equatorial ionosphere-thermosphere system under disturbed conditions, *J. Atmos. Sol. Terr. Phys.*, *59*(13), 1505–1519, doi:10.1016/S1364-6826(96)00152-6.

Anderson, D., A. Anghel, K. Yumoto, M. Ishitsuka, and E. Kudeki (2002), Estimating daytime vertical ExB drift velocities in the equatorial F region using ground-based magnetometer observations, *Geophys. Res. Lett.*, *29*(12), 1596, doi:10.1029/2001GL014562.

Anderson, D., A. Anghel, E. Araujo, V. Eccles, C. Valladares, and C. Lin (2006), Theoretically modeling the low-latitude, ionospheric response to large geomagnetic storms, *Radio Sci.*, *41*, RS5S04, doi:10.1029/2005RS003376.

Basu, S., Su. Basu, F. J. Rich, K. M. Groves, E. MacKenzie, C. Coker, Y. Sahai, P. R. Fagundes, and F. Becker-Guedes (2007), Response of the equatorial ionosphere at dusk to penetration electric fields during intense magnetic storms, *J. Geophys. Res.*, *112*, A08308, doi:10.1029/2006JA012192.

Coster, A. J., M. J. Colerico, J. C. Foster, W. Rideout, and F. Rich (2007), Longitude sector comparisons of storm enhanced density, *Geophys. Res. Lett.*, *34*, L18105, doi:10.1029/2007GL030682.

Crowley, G., et al. (2006), Global Thermosphere-Ionosphere Response to Onset of November 20, 2003 Magnetic Storm, *J. Geophys. Res.*, *111*, A10S18, doi:10.1029/2005JA011518.

de la Beaujardiere, O., J. Watermann, P. Newell, and F. Rich (1993), Relationship between Birkeland current regions, particle precipitation, and electric fields, *J. Geophys. Res.*, *98*(A5), 7711–7720, doi:10.1029/92JA02005.

Fedder, J. A., and J. G. Lyon (1987), The solar wind-magnetosphere-ionosphere current-voltage relationship, *Geophys. Res. Lett.*, *14*(8), 880–883, doi:10.1029/GL014i008p00880.

Fejer, B. G. (2002), Low latitude storm time ionospheric electrodynamics, *J. Atmos. Sol. Terr. Phys.*, *64*, 1401–1408, doi:10.1016/S1364-6826(02)00103-7.

Foster, J. C., and A. J. Coster (2007), Conjugate localized enhancement of total electron content at low latitudes in the American sector, *J. Atmos. Sol. Terr. Phys.*, *69*, 1241–1252, doi:10.1016/j.jastp.2006.09.012.

Fuller-Rowell, T. M., M. V. Codrescu, R. G. Roble, and A. D. Richmond (1997), How does the thermosphere and ionosphere react to a geomagnetic storm?, in *Magnetic Storms*, *Geophys. Monogr. Ser*, vol. 98, edited by B. T. Tsurutani et al., pp. 203–225, AGU, Washington, D. C.

Gonzalez, W. D. (1990), A unified view of solar-wind magnetosphere coupling functions, *Planet. Space Sci.*, *38*(5), 627–632, doi:10.1016/0032-0633(90)90068-2.

Gonzalez, W. D., and B. T. Tsurutani (1987), Criteria of interplanetary parameters causing intense magnetic storms (Dst < 100 nT), *Planet. Space Sci.*, *35*, 1101–1109, doi:10.1016/0032-0633(87)90015-8.

Gonzalez, W. D., B. T. Tsurutani, A. L. C. Gonzalez, E. J. Smith, F. Tang, and S.-I. Akasofu (1989), Solar Wind-Magnetosphere Coupling During Intense Magnetic Storms (1978–1979), *J. Geophys. Res.*, *94*(A7), 8835–8851, doi:10.1029/JA094iA07p08835.

Gonzalez, W. D., J. A. Joselyn, Y. Kamide, H. W. Kroehl, G. Rostoker, B. T. Tsurutani, and V. M. Vasyliunas (1994), What is a geomagnetic storm?, *J. Geophys. Res.*, *99*(A4), 5771–5792, doi:10.1029/93JA02867.

Huang, C.-S., J. C. Foster, and M. C. Kelley (2005), Long-duration penetration of the interplanetary electric field to the low-latitude ionosphere during the main phase of magnetic storms, *J. Geophys. Res.*, *110*, A11309, doi:10.1029/2005JA011202.

Huba, J. D., G. Joyce, S. Sazykin, R. Wolf, and R. Spiro (2005), Simulation study of penetration electric field effects on the low- to mid-latitude ionosphere, *Geophys. Res. Lett.*, *32*, L23101, doi:10.1029/2005GL024162.

Kan, J. R., and L. C. Lee (1979), Energy coupling function and solar wind magnetosphere dynamo, *Geophys. Res. Lett.*, *6*, 577–580, doi:10.1029/GL006i007p00577.

Kelley, M. C., J. J. Makela, J. L. Chau, and M. J. Nicolls (2003), Penetration of the solar wind electric field into the magnetosphere/ionosphere system, *Geophys. Res. Lett.*, *30*(4), 1158, doi:10.1029/2002GL016321.

Komjathy, A., L. Sparks, B. D. Wilson, and A. J. Mannucci (2005), Automated daily processing of more than 1000 ground-based GPS receivers for studying intense ionospheric storms, *Radio Sci.*, *40*, RS6006, doi:10.1029/2005RS003279.

Lin, C. H., A. D. Richmond, J. Y. Liu, H. C. Yeh, L. J. Paxton, G. Lu, H. F. Tsai, and S.-Y. Su (2005a), Large-scale variations of the low-latitude ionosphere during the October–November 2003 superstorm: Observational results, *J. Geophys. Res.*, *110*, A09S28, doi:10.1029/2004JA010900.

Lin, C. H., A. D. Richmond, R. A. Heelis, G. J. Bailey, G. Lu, J. Y. Liu, H. C. Yeh, and S.-Y. Su (2005b), Theoretical study of the low- and midlatitude ionospheric electron density enhancement during the October 2003 superstorm: Relative importance of the neutral wind and the electric field, *J. Geophys. Res.*, *110*, A12312, doi:10.1029/2005JA011304.

Mannucci, A. J., B. D. Wilson, D. N. Yuan, C. M. Ho, U. J. Lindqwister, and T. F. Runge (1998), A global mapping technique for GPS-derived ionospheric total electron content measurements, *Radio Sci.*, *33*(3), 565–582, doi:10.1029/97RS02707.

Mannucci, A. J., B. A. Iijima, U. J. Lindqwister, X. Pi, L. Sparks, and B. D. Wilson (1999), GPS and ionosphere, in *URSI Reviews of Radio Science, 1996–1999*, edited by W. R. Stone, pp. 625–665, Oxford Univ. Press, Oxford, U.K.

Mannucci, A. J., B. T. Tsurutani, B. A. Iijima, A. Komjathy, A. Saito, W. D. Gonzalez, F. L. Guarnieri, J. U. Kozyra, and R. Skoug (2005a), Dayside global ionospheric response to the major interplanetary events of October 29–30, 2003 "Halloween Storms", *Geophys. Res. Lett.*, *32*, L12S02, doi:10.1029/2004GL021467.

Mannucci, A. J., et al. (2005b), Hemispheric Daytime Ionospheric Response To Intense Solar Wind Forcing, in *Inner Magnetosphere Interactions: New Perspectives from Imaging*, *Geophys. Monogr. Ser.*, vol. 159, edited by J. L. Burch, M. Schulz, and H. Spence, AGU, Washington, D.C.

Meier, R. R., G. Crowley, D. J. Strickland, A. B. Christensen, L. J. Paxton, and D. Morrison (2005), First look at the November 20, 2003 super storm with TIMED/GUVI, *J. Geophys. Res.*, *110*, A09S41, doi:10.1029/2004JA010990.

Mendillo, M. (2006), Storms in the ionosphere: Patterns and processes for total electron content, *Rev. Geophys.*, *44*, RG4001, doi:10.1029/2005RG000193.

Newell, P. T., T. Sotirelis, K. Liou, C.-I. Meng, and F. J. Rich (2007), A nearly universal solar wind-magnetosphere coupling function inferred from 10 magnetospheric state variables, *J. Geophys. Res.*, *112*, A01206, doi:10.1029/2006JA012015.

Nopper, R. W., and R. L. Carovillano (1978), Polar-equatorial coupling during magnetically active periods, *Geophys. Res. Lett.*, *5*, 699–702, doi:10.1029/GL005i008p00699.

Prölss, G. W. (1997), Magnetic storm associated perturbations of the upper atmosphere, in *Magnetic Storms*, *Geophys. Monogr. Ser*, vol. 98, edited by B. T. Tsurutani et al., pp. 227–241, AGU, Washington, D. C.

Richmond, A. D. (1995), Ionospheric electrodynamics using magnetic apex coordinates, *J. Geomagn. Geoelectr.*, *47*(2), 191–212.

Richmond, A. D., C. Peymirat, and R. G. Roble (2003), Long-lasting disturbances in the equatorial ionospheric electric field simulated with a

coupled magnetosphere-ionosphere-thermosphere model, *J. Geophys. Res.*, *108*(A3), 1118, doi:10.1029/2002JA009758.

Rothwell, P. L., and J. R. Jasperse (2006), Modeling the connection of the global ionospheric electric fields to the solar wind, *J. Geophys. Res.*, *111*, A03211, doi:10.1029/2004JA010992.

Siscoe, G. L., G. M. Erickson, B. U. Ö. Sonnerup, N. C. Maynard, J. A. Schoendorf, K. D. Siebert, D. R. Weimer, W. W. White, and G. R. Wilson (2002), Hill model of transpolar potential saturation: Comparisons with MHD simulations, *J. Geophys. Res.*, *107*(A6), 1075, doi:10.1029/2001JA000109.

Skoug, R. M., J. T. Gosling, J. T. Steinberg, D. J. McComas, C. W. Smith, N. F. Ness, Q. Hu, and L. F. Burlaga (2004), Extremely high speed solar wind: 29–30 October 2003, *J. Geophys. Res.*, *109*, A09102, doi:10.1029/2004JA010494.

Sonnerup, B. U. O. (1974), agnetopause reconnection rate, *J. Geophys. Res.*, *79*(10), 1546–1549, doi:10.1029/JA079i010p01546.

Tanaka, T., and K. Hirao (1973), Effects of an electric field on the dynamical behavior of the ionospheres and its application to the storm time disturbances of the F-layer, *J. Atmos. Terr. Phys.*, *35*, 1443–1452, doi:10.1016/0021-9169(73)90147-5.

Tsurutani, B. T., W. D. Gonzalez, F. Tang, S. I. Akasofu, and E. J. Smith (1988), Origin of interplanetary southward magnetic-fields responsible for major magnetic storms near solar maximum (1978–1979), *J. Geophys. Res.*, *93*(A8), 8519–8531, doi:10.1029/JA093iA08p08519.

Tsurutani, B. T., et al. (2004), Global dayside ionospheric uplift and enhancement associated with interplanetary electric fields, *J. Geophys. Res.*, *109*, A08302, doi:10.1029/2003JA010342.

Tsurutani, B. T., O. P. Verkhoglyadova, A. J. Mannucci, T. Araki, A. Sato, T. Tsuda, and K. Yumoto (2007), Oxygen ion uplift and satellite drag effects during the 30 October 2003 daytime superfountain event, *Ann. Geophys.*, *25*, 1–6.

Vasyliunas, V. M., J. R. Kan, G. L. Siscoe, and S. I. Akasofu (1982), Scaling relations governing magnetospheric energy-transfer, *Planet. Space Sci.*, *30*(4), 359–365, doi:10.1016/0032-0633(82)90041-1.

Verkhoglyadova, O. P., B. T. Tsurutani, and A. J. Mannucci (2007), Temporal Development Of Dayside Tec Variations During The October 30, 2003 Superstorm: Matching Modeling To Observations, in *Advances in Geosciences, Solar Terrestrial*, vol. 8, edited by M. Duldig, pp. 69–77, World Sci, Hackensack, N. J.

Yizengaw, E., M. B. Moldwin, A. Komjathy, and A. J. Mannucci (2006), Unusual topside ionospheric density response to the November 2003 superstorm, *J. Geophys. Res.*, *111*, A02308, doi:10.1029/2005JA011433.

————————————

M. A. Abdu, E. Echer, and W. D. Gonzalez, National Institute for Space Research, Avenida dos Astronautas 1758, 12201 970, Sao Jose dos Campos, SP, Brazil.

D. Anderson, Space Environment Center, Cooperative Institute for Research in Environmental Science, University of Colorado, 325 Broadway, Boulder, CO 80305, USA.

G. Crowley, Atmospheric and Space Technology Research Associates, 12703 Spectrum Drive, Suite 101, San Antonio, TX 78249, USA.

B. A. Iijima, A. Komjathy, A. J. Mannucci, and B. T. Tsurutani, Jet Propulsion Laboratory, California Institute of Technology, 4800 Oak Grove Drive, MS 138-308, Pasadena, CA 91109, USA. (tony.mannucci@jpl.nasa.gov)